—Original—

Clinicopathological Characteristics of Everolimus-Associated Interstitial Lung Disease: A Single-Center Consecutive Analysis

Yoshinobu Saito[1], Yasuhiro Terasaki[2], Takeru Kashiwada[1], Toru Tanaka[1], Hiroyuki Takei[3], Go Kimura[4], Yukihiro Kondo[4], Tetsuro Kawagoe[5], Akira Matsushita[6], Rintaro Noro[1], Yuji Minegishi[1], Koichiro Kamio[1], Masahiro Seike[1] and Akihiko Gemma[1]

[1]Department of Pulmonary Medicine and Oncology, Nippon Medical School, Tokyo, Japan
[2]Department of Analytic Human Pathology, Nippon Medical School, Tokyo, Japan
[3]Department of Breast Surgery and Oncology, Nippon Medical School, Tokyo, Japan
[4]Department of Urology, Nippon Medical School, Tokyo, Japan
[5]Department of Gastroenterology, Nippon Medical School, Tokyo, Japan
[6]Department of Gastrointestinal and Hepato-Biliary-Pancreatic Surgery, Nippon Medical School, Tokyo, Japan

Background: Everolimus, a mammalian target of rapamycin inhibitor used as an antineoplastic drug, is associated with a remarkably high incidence of interstitial lung disease (ILD). The clinical and pathological characteristics of ILD caused by everolimus have not been thoroughly investigated; therefore, we aimed to elucidate the features of everolimus-associated ILD.

Methods: We retrospectively reviewed the medical records of patients who received everolimus for cancer treatment at our hospital. Patient backgrounds were compared between the ILD and non-ILD groups. Chest computed tomography (CT), changes in biomarkers, and lung histopathological features were analyzed for ILD cases.

Results: Sixty-six patients were reviewed, and ILD developed in 19. There were no differences in patient demographics between the ILD and non-ILD groups. The severity of ILD was grade 1 (G1) in 9 and grade 2 (G2) in 10 cases. Chest CT showed organizing pneumonia (OP) or a hypersensitive pneumonia pattern. The levels of lactate dehydrogenase, C-reactive protein, Krebs von den lungen-6, and surfactant protein-D (SP-D) at the onset of ILD were significantly higher than those at baseline. Analysis of G1 and G2 ILD subgroups showed a higher SP-D levels in the G2 subgroup. Five patients underwent lung biopsies; all specimens demonstrated alveolitis with lymphocytic infiltration and granulomatous lesions, and some had OP findings.

Conclusions: Everolimus-associated ILD is mild and has a favorable prognosis. Patients with symptomatic ILD were more likely to have higher SP-D levels than those with asymptomatic ILD. Granulomatous lesions are an important pathological feature of everolimus-associated ILD.

(J Nippon Med Sch 2024; 91: 207–217)

Key words: everolimus, interstitial lung disease, KL-6, SP-D, granuloma

Introduction

Drug-induced lung diseases present with a wide variety of clinical manifestations, including interstitial lung disease (ILD), a major type of lung disease. Antineoplastic drugs are the most common causative agents of drug-induced ILD, and the frequency and prognosis of drug-induced ILD differ depending on the drug[1].

Everolimus, an inhibitor of mammalian target of rapamycin (mTOR), was first approved as an antineoplastic agent for renal cell carcinoma (RCC), followed by

Correspondence to Yoshinobu Saito, MD, PhD, Department of Pulmonary Medicine and Oncology, Nippon Medical School, 1–1–5 Sendagi, Bunkyo-ku, Tokyo 113–8603, Japan
E-mail: yo-saito@nms.ac.jp
https://doi.org/10.1272/jnms.JNMS.2024_91-211
Journal Website (https://www.nms.ac.jp/sh/jnms/)

neuroendocrine tumor (NET) and breast cancer (BC). It has been noted that everolimus-associated ILD occurs frequently[2], and the incidence of ILD in pivotal clinical trials of everolimus is reported to be 12-17%[3–7]. In our experience, no other drugs induce ILD at such a high frequency, and we have been careful regarding ILD development when everolimus is used for cancer treatment.

There is great interest regarding the clinical features of everolimus-associated ILD, such as its frequency, severity, and prognosis, as well as the utility of diagnostic biomarkers and pathological findings. Details of biomarkers and pathological features of everolimus-associated ILD are particularly scarce. Therefore, we retrospectively reviewed cases that received everolimus for cancer therapy at our hospital and examined the clinical and pathological characteristics of everolimus-associated ILD.

Materials and Methods

Study Participants and Data Collection

We conducted this single-center, retrospective, observational study of everolimus-associated ILD. Ethical approval for this study was obtained from the ethics committee of the Nippon Medical School Hospital (approval number: B-2022-519).

Data of consecutive patients treated with everolimus for RCC, BC, and NET between January 2011 and March 2022 at Nippon Medical School Hospital were analyzed. Data extracted from the medical records included age, sex, performance status, smoking history, allergic history, pre-existing lung disease, type of tumor, symptoms of ILD, laboratory examination, chest computed tomography (CT), bronchoscopy findings, treatment for ILD, and outcome.

Diagnosis and Evaluation of ILD

We investigated the symptoms, chest radiographs, CT scans, and laboratory data of all participants, and everolimus-associated ILD was diagnosed based on the criteria suggested by Camus et al[8]. Briefly, we evaluated each case carefully, considering the temporal relationship between administration and the onset, the differentiation from similar diseases such as infectious disease, congestive heart failure, and lymphangitic carcinomatosis, and then we diagnosed cases with high confidence as everolimus-associated ILD. Chest CT images of ILD were evaluated and classified into five categories, including nonspecific interstitial pneumonia (NSIP), organizing pneumonia (OP), hypersensitivity pneumonia (HP), diffuse alveolar damage (DAD), and eosinophilic pneumonia according to previous literature[9]. ILD severity was graded according to the severity of pneumonitis, as described in the Common Terminology Criteria for Adverse Events version 5.0-JCOG (Japan Clinical Oncology Group). In summary, grade 1 (G1) is asymptomatic, grade 2 (G2) is symptomatic, grade 3 (G3) is severe symptoms, grade 4 is life-threatening, and grade 5 is death[10]. ILD outcomes were assessed using clinical courses and chest imaging.

Statistical Analysis

Data for continuous variables are expressed as median (interquartile range). For two-group comparisons of continuous variables, the Wilcoxon signed-rank test was used for paired group comparisons, and the Mann-Whitney U test was used for unpaired group comparisons. Fisher's exact test was used for two-group comparisons of the categorical variables. Statistical significance was set at $P<0.05$. All statistical analyses were conducted using EZR software (Saitama Medical Center, Jichi Medical University, Saitama, Japan), a graphical user interface for R (The R Foundation for Statistical Computing, Vienna, Austria). More precisely, it is a modified version of the R commander designed to add statistical functions frequently used in biostatistics[11].

Results

Incidence of ILD and Clinical Characteristics of the Study Population

Sixty-six patients treated with everolimus for RCC, BC, or NET were included in this study. Pulmonary opacities were observed in 27 of 66 patients during treatment with everolimus. Of these cases, eight were diagnosed with diseases other than ILD, specifically, lymphangitic carcinomatosis (n=3), lung metastasis (n=1), bacterial pneumonia (n=1), pneumocystis pneumonia (n=1), radiation pneumonitis (n=1), and cardiogenic pulmonary edema (n =1). The remaining 19 (28.8%) patients were diagnosed with everolimus-associated ILD.

The median time to ILD onset from the start of everolimus therapy was 92 days (range: 24-383 days). **Figure 1** shows the cumulative incidence of ILD, which increases linearly over time.

The clinical characteristics of the study population are summarized in **Table 1**. Forty-one cases of BC, 16 cases of RCC, and 9 cases of NET (primary tumor site: pancreas 6, lung 2, and gastrointestinal 1) were included. Six cases exhibited fibrotic changes on chest CT scans taken before everolimus treatment. Of these, 4 had slight reticular abnormalities in the subpleural regions of bilateral

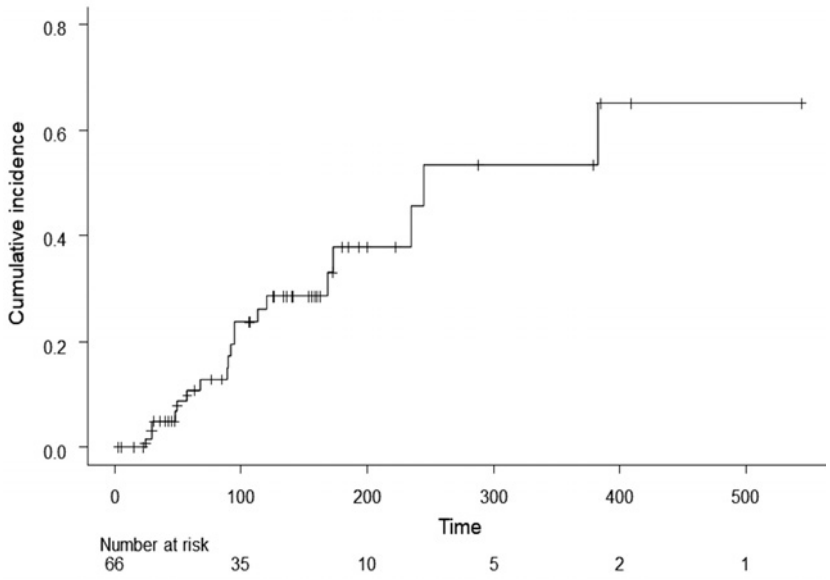

Fig. 1 Cumulative incidence of ILD after the start of everolimus therapy.
ILD, interstitial lung disease.

Table 1 Baseline characteristics of patients who received everolimus therapy

	Total (n=66)	ILD (n=19)	non-ILD (n=47)	P value
Age, median (IQR)	64 (51.25-72.25)	62 (52-70.5)	64 (51-73)	0.955
Sex, Male; n (%)	20 (30.3)	6 (31.6)	14 (29.8)	1
Current or former smoker, n (%)	32 (48.5)	7 (36.8)	25 (53.2)	0.352
Allergic history, n (%)	21 (31.8)	9 (47.4)	12 (25.5)	0.152
Tumor, n (%)				1
BC	41 (62.1)	12 (63.2)	29 (61.7)	
RCC	16 (24.2)	5 (26.3)	11 (23.4)	
NET	9 (13.6)	2 (10.5)	7 (14.9)	
ECOG-PS, n (%)				0.316
0-1	62 (93.9)	19 (100)	43 (91.5)	
≥ 2	4 (6.1)	0 (0)	4 (8.5)	
Pre-existing lung disease, n (%)				
Fibrotic changes	6 (9.1)	0 (0)	6 (12.8)	0.171
Pulmonary metastasis	29 (43.9)	7 (36.8)	22 (46.8)	0.584
Emphysema	6 (9.1)	1 (5.3)	5 (10.6)	0.664
Pleural effusion	13 (19.7)	5 (26.3)	8 (17.0)	0.496
Laboratory data, median (IQR)				
WBC (/μL)	4,600 (3,550-6,475)	4,300 (3,300-5,900)	4,700 (3,800-6,600)	0.661
LDH (U/L)	202.5 (184.25-249.5)	198 (187-237.5)	205 (183.5-255)	0.810
CRP (mg/dL)	0.26 (0.0825-0.96)	0.20 (0.07-0.76)	0.27 (0.09-0.94)	0.707
Alb (g/dL)	4.1 (3.7-4.4)	4.3 (3.85-4.5)	4.0 (3.7-5.2)	0.196
eGFR (mL/min/1.73 m^2)	63 (54-77.75)	63 (49.5-73)	67 (54-79)	0.470
KL-6 (U/mL)	525.8 (295.225-1,531.5)	405.2 (265.0-1,462.45)	595.1 (329.325-1,531.5)	0.737
SP-D (ng/mL)	45.2 (21.75-78.1)	38.5 (25.85-55.2)	46.0 (20.675-91.4)	0.484

IQR, interquartile range; BC, breast cancer; RCC, renal cell carcinoma; NET, neuroendocrine tumor; ECOG-PS, Eastern Cooperative Oncologic Group Performance Status; WBC, white blood cells; LDH, lactate dehydrogenase; CRP, C-reactive protein; Alb, albumin; eGFR, estimated glomerular filtration rate; KL-6, Krebs von den lungen-6; SP-D, surfactant protein-D.

lower lungs and 2 had subpleural fibrotic changes confined to a narrow area in the right upper lobe, which was caused by tangential irradiation for BC. Age, sex, smoking history, allergic history, tumor type, Eastern Co-

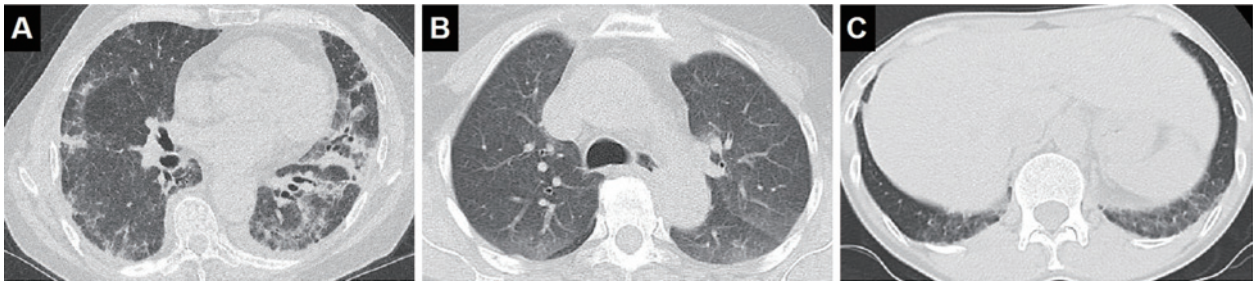

Fig. 2 Chest CT images of the ILD cases.
A) Bilateral ground-glass opacities and focal areas of consolidation are mainly in the peribronchial and subpleural regions, representing the OP pattern. B) Patchy ground-glass opacities in bilateral lungs indicate the HP pattern. C) Reticular shadows superimposed on mild ground-glass opacities in the bilateral basal lungs are consistent with the NSIP pattern.
ILD, interstitial lung disease; CT, computed tomography; OP, organizing pneumonia; HP, hypersensitivity pneumonia; NSIP, nonspecific interstitial pneumonia.

operative Oncology Group-Performance Status, preexisting lung diseases, and baseline laboratory data were not significantly different between the ILD and non-ILD groups.

Severity and Subjective Symptoms of ILD

Among the 19 ILD cases, 9 were of G1, 10 were of G2, and none were G3 or higher. Regarding ILD severity according to tumors, four cases of G1 ILD and one case of G2 ILD developed in patients with RCC. Four cases of G1 ILD and eight cases of G2 ILD developed in patients with BC. In addition, one patient with pancreatic NET developed G1 ILD, and one with pulmonary NET developed G2 ILD. No significant differences in patient background were observed between G1 and G2 ILD patients.

Various subjective symptoms were observed in patients with G2 ILD. Cough was observed in 10 patients, of which 6 had a dry cough, and 4 had a productive cough. In addition, dyspnea was observed in six cases, fever in four cases, and malaise in one case.

Radiographical Findings

Chest CT findings at the time of ILD diagnosis showed bilateral opacities in 16 cases and unilateral opacities in 3 cases. Regarding ILD pattern classification, there were 10 cases of the OP pattern, 8 cases of the HP pattern, and 1 case of the NSIP pattern. There was no difference in CT pattern between G1 and G2 ILD. **Figure 2** shows the representative CT scans for each pattern.

Biomarkers Associated with ILD

Figure 3A compares white blood cell count, lactate dehydrogenase (LDH), C-reactive protein (CRP), Krebs von den lungen-6 (KL-6), and surfactant protein-D (SP-D) levels between the baseline and at the ILD onset. The LDH, CRP, KL-6, and SP-D levels at the onset of ILD were significantly higher than those at baseline (P=0.000143, P=0.0204, P=0.0000305, and P=0.00836, respectively). Serum KL-6 level could be elevated in BC patients as a tumor marker, and subgroup analyses were also conducted. The KL-6 levels were significantly higher at the onset of ILD in both BC and non-BC groups (P=0.00391 and P=0.01563, respectively; **Supplementary Fig. 1**: https://doi.org/10.1272/jnms.JNMS.2024_91-211).

Furthermore, we examined the relationship between the severity at the onset of ILD and these biomarkers. At the onset of ILD, the level of WBC, LDH, and CRP were not significantly different between G1 and G2 ILD cases [4,300 (3,400-5,100) vs. 4,350 (3,725-5,025)/μL, P = 0.902; 310.5 (239.5-395.75) vs. 321.0 (301.0-348.0) U/L, P = 0.815; 1.545 (0.910-3.4475) vs. 1.000 (0.595-3.7850) mg/dL, P = 0.778, respectively]. On the other hand, the level of SP-D was significantly higher in G2 than in G1 ILD cases [126.75 (104.375-140.825) vs. 57.20 (24.175-100.375) ng/mL, P = 0.0499], and analysis by severity revealed that G2 ILD cases had significantly higher SP-D levels at the onset of ILD compared to baseline (P=0.0156), while no significant difference was observed in G1 ILD cases (P=0.469) (**Fig. 3B**). Regarding KL-6, G2 ILD cases included more BC patients than G1 ILD, and some of these patients could have elevated KL-6 as a tumor marker. Therefore, comparisons between G1 and G2 ILD cases were not conducted.

Bronchoalveolar Lavage and Transbronchial Lung Biopsy Findings

Bronchoscopy was performed for diagnosis in five cases. All patients showed a marked increase in lymphocyte fractionation in bronchoalveolar lavage (BAL) fluid analysis. Eosinophil fractions mildly increased in some patients. The CD4/CD8 ratio of lymphocytes in BAL fluid ranged from 2.0 to 7.2, and four out of five cases

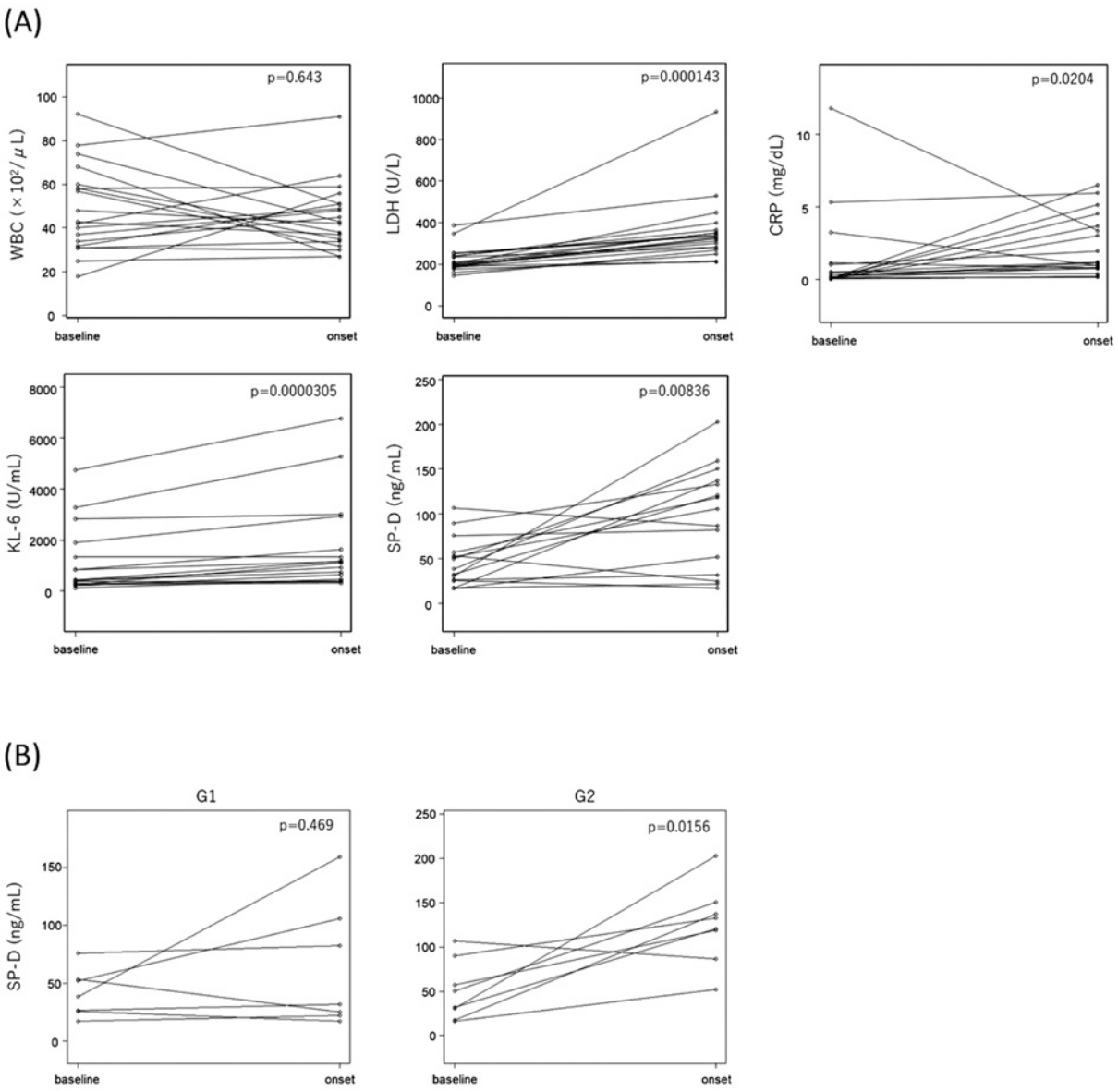

Fig. 3 A) Comparison of WBC, LDH, CRP, KL-6, and SP-D levels between baseline and at the onset of the ILD. B) Comparison of SP-D levels between baseline and at the onset of the ILD in G1 and G2 ILD subgroups.
WBC, white blood cells; LDH, lactate dehydrogenase; CRP, C-reactive protein; KL-6, Krebs von den lungen-6; SP-D, surfactant protein-D; ILD, interstitial lung disease.

Table 2 BAL fluid analyses in 5 cases at the diagnosis of ILD

Case No.	TCC (×10⁵/mL)	M (%)	Lym (%)	Neu (%)	Eos (%)	CD4/CD8	CT pattern
1	7.9	8	80	0	12	2	OP
2	12.7	32.5	67.5	0	0	5.4	NSIP
3	17.5	6	94	0	0	4.8	OP
4	N.A.	2	96	0	2	7.2	OP
5	3.8	13	66	6	15	4.5	HP

TCC, total cell count; M, macrophages; Lym, lymphocytes; Neu, neutrophils; Eos, eosinophils; N.A., not assessed.

showed an elevation of the ratio (**Table 2**).

Histopathological findings of the transbronchial lung biopsy specimens demonstrated cellular and myxomatous alveolitis with infiltration of inflammatory cells,

mainly lymphocytes. All cases presented with either granuloma formation or granulomatous changes in the lesion (**Fig. 4**). Two cases were accompanied by intra-alveolar polypoid fibrosis and collagen globules, which suggested OP. **Figure 5** shows histopathological images of OP findings as a representative case.

Treatment and Outcomes of ILD

Corticosteroids were administered to 6 of 10 G2 ILD cases and 1 of 9 G1 ILD cases; the other cases were untreated. The corticosteroid administered was 0.5 mg/kg of prednisolone in each case. The median duration of corticosteroid treatment was 27 (22-57.5) days. The outcomes were as follows: ILD recovered in 18 cases and did not recover in 1 case. The patient who did not recover died of cancer progression shortly after the ILD diagnosis. In one G1 and six G2 cases, everolimus was resumed after the interruption [the median interruption period was 32 (20.5-42.5) days], but no recurrence of ILD was observed. Five patients with G1 ILD continued receiving everolimus without worsening the severity. One patient with G2 ILD had very mild symptom and continued to receive everolimus without interruption. However, the ILD did not worsen and recovered soon after discontinuation of everolimus due to progressive disease. In a total of 6 patients, 3 in G1 and 3 in G2, everolimus was permanently discontinued at the onset of ILD because of progressive disease or anorexia.

Discussion

Herein, ILD developed in 28.8% of patients treated with everolimus. The incidence was higher than that in clinical trials of everolimus, such as the RECORD-1, RADIANT-3, and BOLERO-2 studies[3,4,7]; however, it was similar to the incidence of ILD in the Japanese population in each study[12–14]. It has been reported that Japanese people are more likely to develop drug-induced ILD with several drugs[15–17], which might be true for everolimus-associated ILD. The severity of ILD was mild, and no one developed G3 or higher ILD in our study population. In clinical trials, 3-5% of patients developed G3 or higher ILD[3,4,7]. Although the reason for the absence of severe cases in our study was unknown, it may have been because of the small number of cases herein. The time to onset of ILD ranged widely from 24 to 383 days, and the cumulative incidence curve showed a linear increase, suggesting that everolimus-associated ILD did not tend to occur at a particular period, and that the development of ILD should be monitored throughout everolimus therapy. We compared the background factors between the ILD and non-ILD groups; however, no differences were found between the two groups. Therefore, we could not estimate the risk factors for ILD development in patients treated with everolimus. Pre-existing ILD is a well-known risk factor for drug-induced lung injury[9]. Six patients had pre-existing fibrotic changes in the lungs before treatment with everolimus. However, none of them developed everolimus-induced ILD during their clinical course. The stable clinical course despite everolimus administration may be attributed to the mild or localized nature of fibrotic changes in these cases. However, due to the small number of cases in this study, it is not possible to conclude that everolimus is safe for cases with mild pre-existing fibrotic changes. Moreover, everolimus has been shown to worsen the progression of pulmonary fibrosis in a clinical trial of advanced pulmonary fibrosis[18]. Therefore, administration of everolimus should be avoided in cases with advanced pulmonary fibrosis. Concerning the management of ILD, the package insert for everolimus allows treatment to continue in the case of G1 ILD and resume treatment after the ILD has resolved in the case of G2 ILD. These guidelines were reconfirmed as safe in this study; however, in such cases, the continuation of everolimus for G1 ILD and re-administration after the resolution of G2 ILD should be monitored carefully.

Biomarkers used to diagnose drug-induced ILD include complete blood count, LDH, CRP, and alveolar epithelial cell markers such as KL-6 and SP-D[9]. KL-6 and SP-D are derived from type II alveolar epithelial cells, and their serum levels are higher in patients with ILD than in healthy participants[19,20]. In this study, the levels of nonspecific inflammatory markers LDH and CRP, as well as alveolar epithelial markers KL-6 and SP-D, were elevated at the onset of ILD. We examined the relationship between ILD severity and SP-D levels; the levels at the onset of ILD was higher in G2 ILD cases than in G1 ILD cases for SP-D. Furthermore, from baseline to the onset of ILD, SP-D levels increased significantly in G2 ILD cases, but no significant increase was observed in G1 ILD cases. There may be a correlation between the degree of lung injury and the presence or absence of symptoms. In addition, if the lung injury is severe, more SP-D released from the damaged type II alveolar epithelial cells could flow into the blood vessels, resulting in increased serum levels of SP-D. KL-6 is a useful biomarker for diagnosing ILD; however, it is also a tumor marker for BC patients, especially in advanced cases[21]. Therefore, KL-6 levels could be influenced by tumor status and should be interpreted with caution. In the case of BC, chest CT scans,

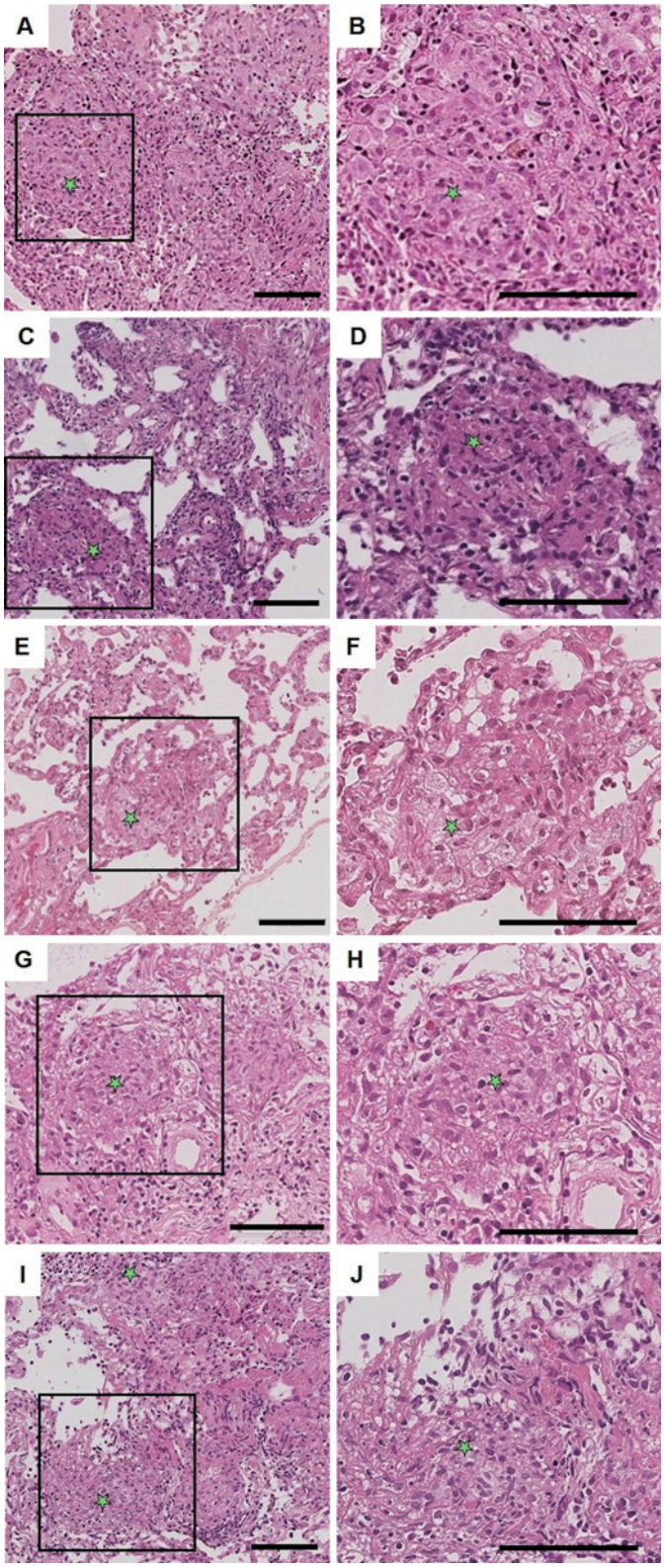

Fig. 4 TBLB specimens from five patients with everolimus-associated ILD.
A), C), E), G), and I) shows middle-power views of Case No. 1, 2, 3, 4, and 5, respectively. The areas enclosed by black rectangles indicate granulomatous lesions (green star) as epithelioid histiocyte accumulation, and their high-magnification views are shown on the right (B, D, F, H, and J). Scale bars = 100 μm.
ILD, interstitial lung disease.

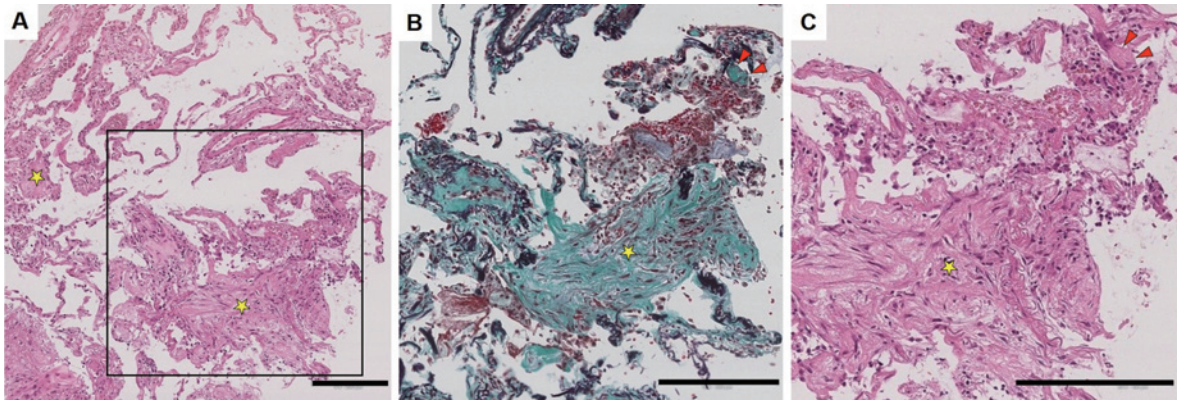

Fig. 5 Histopathological findings suggesting an OP pattern of the lung lesion.
A) Middle-power view of a specimen (Case No. 3). Diffuse cellular and fibrous thickening of the alveolar wall with myxofibrous organized lesions (yellow stars). B, C) Intra-alveolar fibrous lesion (yellow star) with collagen globule (red arrowheads). The black rectangle in (A) indicates a high-magnification view of the area. H&E (A, C) and Elastica Masson-Goldner (B) staining. Scale bars = 200 μm.
H&E, hematoxylin and eosin; OP, organizing pneumonia.

tumor marker changes, and results of physical examination and breast ultrasonography by a breast surgeon are checked. From this information, we determine whether the BC is progressing or not, and ultimately determine whether the increase in KL-6 value is due to tumor worsening or ILD. This is the process of diagnostic work-up for evaluating KL-6 levels in BC cases. When using KL-6 to monitor ILD, baseline KL-6 levels should be measured, and if KL-6 levels rise above baseline, the possibility of tumor progression, as well as ILD development, should be considered.

The CT images of drug-induced ILD are often recognized as patterns. In other words, it is expressed as patterns similar to those of other ILDs, such as OP, NSIP, eosinophilic pneumonia, HP, and acute interstitial pneumonia/DAD, rather than CT findings, such as ground-glass opacity, consolidation, and nodules. In this study, most patients had OP or HP patterns, which are generally considered responsive to corticosteroids and have a better prognosis; the DAD pattern was not observed. DAD, the pathology of acute respiratory distress syndrome or acute interstitial pneumonia, is a serious condition with a high mortality rate. Studies of Japanese post-marketing surveillance for some tyrosine kinase inhibitors and an immune checkpoint inhibitor investigated the CT pattern and prognosis in ILD and showed a very high mortality rate ranging from 53 to 75% in cases with a DAD pattern[22–26]. The CT patterns of everolimus-associated ILD show mainly OP, NSIP, and HP patterns[27,28], and the DAD pattern is rare. It is considered one of the factors for a favorable prognosis.

ILD is a common adverse event associated with everolimus treatment in cancer patients. However, there are very few detailed reports on the histopathological findings, and the pathological features of everolimus-associated ILD have not yet been fully elucidated. Thirteen reports mentioned the pathological findings of everolimus-associated ILD, of which 10 were single-case studies, 2 were 2-case studies, and 1 was a 3-case study[2,29–40]. Summarizing these reports of 17 cases, alveolitis with lymphocytic infiltration and OP were the main pathological findings, except for one case of diffuse alveolar hemorrhage[38]. In particular, OP findings were reported in 8 out of 17 cases[2,29–31,36,39,40]. In our study, a case series of five patients also showed alveolitis with lymphocytic infiltration, and OP findings accompanied two cases. It should be noted that all cases had granulomatous lesions. Granulomatous lesions were reported in 4 of the 17 cases[2,37,39,40]; one of these previously reported cases[37] was included in the five cases in this study. Considering our data and previous reports, granulomatous lesions are an important pathological characteristic of everolimus-associated ILD, in addition to cellular alveolitis with lymphocytic infiltration and occasional OP findings.

HP is a typical ILD accompanied by granuloma formation. However, among the five cases, only one case (case No. 5) had the HP pattern, the other three cases had OP pattern, and one case had NSIP pattern. It has been reported that CT patterns and histopathological findings of lung biopsies are often inconsistent[41]. Transbronchial lung biopsy findings represent only a biopsied part and may not reflect the complete histopathological changes. In

drug-induced lung injury, multiple and mixed histopathological findings can be observed within the same lung[9]. In contrast, when classifying CT findings into patterns, they are evaluated as a whole image and classified into single pattern such as OP, HP, NSIP, and DAD based on comparison with imaging patterns of idiopathic forms[42]. Therefore, pathological patterns inferred from histopathological findings obtained from very small tissues may not necessarily match CT patterns.

It is interesting why everolimus-associated ILD is prone to granulomatous lesion development. Several reports have discussed the relationship between mTOR signaling and granuloma formation. Linke et al[43]. reported that granulomas spontaneously developed in the lungs and livers of mice in which the tuberous sclerosis complex type 2 gene was deleted, and mTORC1 was activated. However, the granulomas disappeared after the administration of everolimus. This result contradicts the findings of the present study. However, the pathogenesis of mTOR inhibitor-induced granuloma formation in humans is complicated and may involve a variety of effects different from the granuloma formation seen in tuberous sclerosis complex type 2 knockout mice, considering other reports investigating mTORC1 signaling using different mouse models of granuloma formation. For example, we previously reported that the expression of peroxisome proliferator-activated receptor gamma (PPARγ) was decreased in the lung tissues of mouse models of pneumonitis caused by an mTOR inhibitor[44], which is consistent with reports stating that the expression of PPARγ could be induced by mTORC1 signaling[45,46]. Furthermore, using a nanotube-elicited granulomatous lung inflammation model, macrophage-specific PPARγ knockout conditional mice formed more extensive granulomatous lesions than wild-type mice, and PPARγ-specific ligands attenuated granuloma formation[47,48]. These findings support the hypothesis that suppression of PPARγ by mTOR inhibitors may facilitate the development of granulomatous lesions in everolimus-associated ILD, as observed in our results.

This study has some limitations. First, this was a retrospective observational study at a single institution; thus, there was a possibility of selection bias, and missing values were unavoidable in data collection. In this study, data of all patients treated with everolimus were reviewed, and the study period was set so that consecutive cases in which treatment was completed were included. Although this minimized the selection bias within the institution, there may be other potential biases. For example, because the frequency of chest CT scans was not standardized, there may have been ILD cases that had not been detected.

Regarding the issue of missing data, only a small number of missing data were found regarding the biomarkers analyzed in this study. However, it is essential to acknowledge that missing data could potentially impact the study results, and caution should be exercised when interpreting the findings. Second, the number of cases investigated in this study was 66, and the sample size was small. In addition, only five patients underwent lung biopsy, which is a small number to elucidate the pathological features. However, the fact that granulomatous lesions were observed in all cases suggests that it may be a pathological characteristic of everolimus-associated ILD; further confirmation in future studies is needed. To overcome these limitations, well-designed prospective observational studies with sufficient cases are required.

In conclusion, everolimus frequently causes ILD in patients undergoing cancer treatment; however, most cases are mild and have a favorable prognosis. Granulomatous lesions are an important characteristic pathological feature of everolimus-associated ILD, in addition to cellular alveolitis with lymphocytic infiltration and occasional OP findings. These pathological features of ILD are likely related to good steroid responsiveness and a favorable clinical course.

Acknowledgments: We would like to thank all physicians and medical staff who were engaged in the treatment and care for the study participants. We would like to thank Editage (www.editage.com) for English language editing.

Funding: This research did not receive specific grants from public, commercial, or not-for-profit funding agencies.

Conflict of Interest: All authors have no conflict of interest with regards to this paper.

References

1. Saito Y, Gemma A. Current status of DILD in molecular targeted therapies. Int J Clin Oncol. 2012 Dec;17(6):534–41.
2. White DA, Camus P, Endo M, et al. Noninfectious pneumonitis after everolimus therapy for advanced renal cell carcinoma. Am J Respir Crit Care Med. 2010 Aug 1;182 (3):396–403.
3. Motzer RJ, Escudier B, Oudard S, et al. Phase 3 trial of everolimus for metastatic renal cell carcinoma: final results and analysis of prognostic factors. Cancer. 2010 Sep 15;116(18):4256–65.
4. Yao JC, Shah MH, Ito T, et al. Everolimus for advanced

pancreatic neuroendocrine tumors. N Engl J Med. 2011 Feb 10;364(6):514–23.
5. Pavel ME, Hainsworth JD, Baudin E, et al. Everolimus plus octreotide long-acting repeatable for the treatment of advanced neuroendocrine tumours associated with carcinoid syndrome (RADIANT-2): a randomised, placebo-controlled, phase 3 study. Lancet. 2011 Dec 10;378(9808): 2005–12.
6. Yao JC, Fazio N, Singh S, et al. Everolimus for the treatment of advanced, non-functional neuroendocrine tumours of the lung or gastrointestinal tract (RADIANT-4): a randomised, placebo-controlled, phase 3 study. Lancet. 2016 Mar 5;387(10022):968–77.
7. Baselga J, Campone M, Piccart M, et al. Everolimus in postmenopausal hormone-receptor-positive advanced breast cancer. N Engl J Med. 2012 Feb 9;366(6):520–9.
8. Camus P, Fanton A, Bonniaud P, Camus C, Foucher P. Interstitial lung disease induced by drugs and radiation. Respiration. 2004 Jul-Aug;71(4):301–26.
9. Kubo K, Azuma A, Kanazawa M, et al. Consensus statement for the diagnosis and treatment of drug-induced lung injuries. Respir Investig. 2013 Dec;51(4):260–77.
10. Japan Clinical Oncology Group. Common Terminology Criteria for Adverse Events (CTCAE) version 5.0-JCOG [Internet]. Tokyo: Japan Clinical Oncology Group; 2022 Sep 5 [cited 2023 Aug 1]. Available from: https://jcog.jp/doctor/tool/ctcaev5
11. Kanda Y. Investigation of the freely available easy-to-use software 'EZR' for medical statistics. Bone Marrow Transplant. 2013 Mar;48(3):452–8.
12. Tsukamoto T, Shinohara N, Tsuchiya N, et al. Phase III trial of everolimus in metastatic renal cell carcinoma: subgroup analysis of Japanese patients from RECORD-1. Jpn J Clin Oncol. 2011 Jan;41(1):17–24.
13. Ito T, Okusaka T, Ikeda M, et al. Everolimus for advanced pancreatic neuroendocrine tumours: a subgroup analysis evaluating Japanese patients in the RADIANT-3 trial. Jpn J Clin Oncol. 2012 Oct;42(10):903–11.
14. Ito Y, Masuda N, Iwata H, et al. Everolimus plus exemestane in postmenopausal patients with estrogen-receptor-positive advanced breast cancer - Japanese subgroup analysis of BOLERO-2. Gan To Kagaku Ryoho. 2015 Jan; 42(1):67–75.
15. Azuma A, Kudoh S. High prevalence of drug-induced pneumonia in Japan. JMAJ [Internet]. 2007 [cited 2023 Aug 1];50(5):405–11. Available from: https://www.med.or.jp/english/activities/pdf/jmaj/v50no05.pdf
16. Suh CH, Park HS, Kim KW, Pyo J, Hatabu H, Nishino M. Pneumonitis in advanced non-small-cell lung cancer patients treated with EGFR tyrosine kinase inhibitor: meta-analysis of 153 cohorts with 15,713 patients: meta-analysis of incidence and risk factors of EGFR-TKI pneumonitis in NSCLC. Lung Cancer. 2018 Sep;123:60–9.
17. Powell CA, Modi S, Iwata H, et al. Pooled analysis of drug-related interstitial lung disease and/or pneumonitis in nine trastuzumab deruxtecan monotherapy studies. ESMO Open. 2022 Aug;7(4):100554.
18. Malouf MA, Hopkins P, Snell G, Glanville AR; Everolimus in IPF Study Investigators. An investigator-driven study of everolimus in surgical lung biopsy confirmed idiopathic pulmonary fibrosis. Respirology. 2011 Jul;16(5): 776–83.
19. Kohno N, Kyoizumi S, Awaya Y, Fukuhara H, Yamakido M, Akiyama M. New serum indicator of interstitial pneumonitis activity. Sialylated carbohydrate antigen KL-6. Chest. 1989 Jul;96(1):68–73.
20. Honda Y, Kuroki Y, Matsuura E, et al. Pulmonary surfactant protein D in sera and bronchoalveolar lavage fluids. Am J Respir Crit Care Med. 1995 Dec;152(6 Pt 1):1860–6.
21. Ogawa Y, Ishikawa T, Ikeda K, et al. Evaluation of serum KL-6, a mucin-like glycoprotein, as a tumor marker for breast cancer. Clin Cancer Res. 2000 Oct;6(10):4069–72.
22. Horiuchi-Yamamoto Y, Gemma A, Taniguchi H, et al. Drug-induced lung injury associated with sorafenib: analysis of all-patient post-marketing surveillance in Japan. Int J Clin Oncol. 2013 Aug;18(4):743–9.
23. Gemma A, Kusumoto M, Kurihara Y, et al. Interstitial lung disease onset and its risk factors in Japanese patients with ALK-positive NSCLC after treatment with crizotinib. J Thorac Oncol. 2019 Apr;14(4):672–82.
24. Gemma A, Kusumoto M, Sakai F, et al. Real-world evaluation of factors for interstitial lung disease incidence and radiologic characteristics in patients with EGFR T790M-positive NSCLC treated with osimertinib in Japan. J Thorac Oncol. 2020 Dec;15(12):1893–906.
25. Saito Y, Sasaki S, Oikado K, et al. Radiographic features and poor prognostic factors of interstitial lung disease with nivolumab for non-small cell lung cancer. Cancer Sci. 2021 Apr;112(4):1495–505.
26. Chen Y, Noma S, Taguchi Y, et al. Characteristics of interstitial lung disease in patients from post-marketing data on metastatic breast cancer patients who received abemaciclib in Japan. Breast Cancer. 2021 May;28(3):710–9.
27. Nishino M, Boswell EN, Hatabu H, Ghobrial IM, Ramaiya NH. Drug-related pneumonitis during mammalian target of rapamycin inhibitor therapy: radiographic pattern-based approach in waldenstrom macroglobulinemia as a paradigm. Oncologist. 2015 Sep;20(9):1077–83.
28. Nishino M, Brais LK, Brooks NV, Hatabu H, Kulke MH, Ramaiya NH. Drug-related pneumonitis during mammalian target of rapamycin inhibitor therapy in patients with neuroendocrine tumors: a radiographic pattern-based approach. Eur J Cancer. 2016 Jan;53:163–70.
29. Rothenburger M, Zuckermann A, Bara C, et al. Recommendations for the use of everolimus (Certican) in heart transplantation: results from the second German-Austrian Certican Consensus Conference. J Heart Lung Transplant. 2007 Apr;26(4):305–11.
30. O'Donnell A, Faivre S, Burris HA 3rd, et al. Phase I pharmacokinetic and pharmacodynamic study of the oral mammalian target of rapamycin inhibitor everolimus in patients with advanced solid tumors. J Clin Oncol. 2008 Apr 1;26(10):1588–95.
31. Exposito V, de Prada JA, Gomez-Roman JJ, et al. Everolimus-related pulmonary toxicity in heart transplant recipients. J Heart Lung Transplant. 2008 Jul;27(7):797–800.
32. Alexandru S, Ortiz A, Baldovi S, et al. Severe everolimus-associated pneumonitis in a renal transplant recipient. Nephrol Dial Transplant. 2008 Oct;23(10):3353–5.
33. Schrader J, Sterneck M, Klose H, Lohse AW, Nashan B, Fischer L. Everolimus-induced pneumonitis: report of the first case in a liver transplant recipient and review of treatment options. Transpl Int. 2010 Jan;23(1):110–3.
34. Mizuno R, Asano K, Mikami S, Nagata H, Kaneko G, Oya M. Patterns of interstitial lung disease during everolimus treatment in patients with metastatic renal cell carcinoma. Jpn J Clin Oncol. 2012 May;42(5):442–6.
35. Sakamoto S, Kikuchi N, Ichikawa A, et al. Everolimus-induced pneumonitis after drug-eluting stent implantation: a case report. Cardiovasc Intervent Radiol. 2013 Aug;36(4):1151–4.

36. Lanfranco J, Holt A, Montague A, Oza TH, Elballat M, Romero-Legro IH. Everolimus induced organizing pneumonia in a patient with tuberous sclerosis complex. Respir Med Case Rep. 2021 Jan 24;32:101347.
37. Saito Y, Kunugi S, Suzuki Y, et al. Granuloma-forming interstitial pneumonia occurring one year after the start of everolimus therapy. Intern Med. 2013;52(2):263–7.
38. Vandewiele B, Vandecasteele SJ, Vanwalleghem L, De Vriese AS. Diffuse alveolar hemorrhage induced by everolimus. Chest. 2010 Feb;137(2):456–9.
39. Nazer L, Alnajjar T, Salah S, Khzouz J, Alfaqeer N, Qandeel M. Fatal case of cryptogenic organizing pneumonia associated with everolimus. Ann Saudi Med. 2014 Sep-Oct;34(5):437–9.
40. Kim CJ, McKenzie D, Joseph JK, et al. Refractory metastatic insulinoma treated with everolimus, complicated by cryptogenic organizing pneumonia. Am J Med Case Rep [Internet]. 2019 Jun [cited 2023 Aug 1];7(7):125–32. Available from: http://www.sciepub.com/AJMCR/content/7/7
41. Cleverley JR, Screaton NJ, Hiorns MP, Flint JD, Muller NL. Drug-induced lung disease: high-resolution CT and histological findings. Clin Radiol. 2002 Apr;57(4):292–9.
42. Sakai F, Johkoh T, Kusumoto M, Arakawa H, Takahashi M. Drug-induced interstitial lung disease in molecular targeted therapies: high-resolution CT findings. Int J Clin Oncol. 2012 Dec;17(6):542–50.
43. Linke M, Pham HT, Katholnig K, et al. Chronic signaling via the metabolic checkpoint kinase mTORC1 induces macrophage granuloma formation and marks sarcoidosis progression. Nat Immunol. 2017 Mar;18(3):293–302.
44. Kokuho N, Terasaki Y, Kunugi S, et al. Analyses of alveolar epithelial injury via lipid-related stress in mammalian target of rapamycin inhibitor-induced lung disease. Lab Invest. 2019 Jun;99(6):853–65.
45. Kim JE, Chen J. Regulation of peroxisome proliferator-activated receptor-gamma activity by mammalian target of rapamycin and amino acids in adipogenesis. Diabetes. 2004 Nov;53(11):2748–56.
46. Kang S, Nakanishi Y, Kioi Y, et al. Semaphorin 6D reverse signaling controls macrophage lipid metabolism and anti-inflammatory polarization. Nat Immunol. 2018 Jun;19(6):561–70.
47. Huizar I, Malur A, Patel J, et al. The role of PPARγ in carbon nanotube-elicited granulomatous lung inflammation. Respir Res. 2013 Jan 23;14(1):7.
48. McPeek M, Malur A, Tokarz DA, Murray G, Barna BP, Thomassen MJ. PPAR-gamma pathways attenuate pulmonary granuloma formation in a carbon nanotube induced murine model of sarcoidosis. Biochem Biophys Res Commun. 2018 Sep 5;503(2):684–90.

(Received, August 4, 2023)
(Accepted, November 22, 2023)
(J-STAGE Advance Publication, January 16, 2024)